

Copyright © 1993, by the author(s).  
All rights reserved.

Permission to make digital or hard copies of all or part of this work for personal or classroom use is granted without fee provided that copies are not made or distributed for profit or commercial advantage and that copies bear this notice and the full citation on the first page. To copy otherwise, to republish, to post on servers or to redistribute to lists, requires prior specific permission.

**TIME SCALE TO ERGODICITY IN THE FPU  
SYSTEM**

by

J. De Luca, A. J. Lichtenberg, and M. A. Lieberman

Memorandum No. UCB/ERL M93/92

15 November 1993

*Handwritten:*  
C. W. ...  
M. A. ...

**TIME SCALE TO ERGODICITY IN THE FPU  
SYSTEM**

by

J. De Luca, A. J. Lichtenberg, and M. A. Lieberman

Memorandum No. UCB/ERL M93/92

15 November 1993

**ELECTRONICS RESEARCH LABORATORY**

College of Engineering  
University of California, Berkeley  
94720

**TIME SCALE TO ERGODICITY IN THE FPU  
SYSTEM**

by

J. De Luca, A. J. Lichtenberg, and M. A. Lieberman

Memorandum No. UCB/ERL M93/92

15 November 1993

**ELECTRONICS RESEARCH LABORATORY**

College of Engineering  
University of California, Berkeley  
94720

## Time Scale to Ergodicity in the FPU System

J. De Luca<sup>†</sup>, A. J. Lichtenberg<sup>†</sup> and M. A. Lieberman<sup>†</sup>

Department of Electrical Engineering and Computer Sciences<sup>†</sup>  
and Department of Physics<sup>†</sup>  
University of California, Berkeley CA, 94720

Received(

We study the approach to near-equipartition in an  $N$ -dimensional FPU Hamiltonian. We investigate numerically the time evolution of orbits with initial energy in some few low-frequency linear modes. Our results indicate a transition where, above a critical energy, one can reach near-equipartition if one waits for a time proportional  $N^2$ . Below this critical energy the time is exponentially long. We develop a theory to understand the time evolution and deformation of the actions of the oscillators based on a normal form treatment of the resonances among the oscillators. Our theory predicts the critical energy for near-equipartition, the time scale to near-equipartition and the deformation of the actions below equipartition, in qualitative agreement with the numerical results.

# 1 Introduction

There have been many studies of the “equipartition threshold” in the FPU system. Fermi, Pasta and Ulam(FPU)[1] in 1954, performed the first numerical study on a chain of nonlinear oscillators observing, for a particular initial energy distribution, that the oscillators did not relax to the equipartition state, but displayed a persistent recurrence to the initial condition, contrary to the equipartition hypothesis of statistical mechanics. Their results were later reproduced by Tuck and Menzel[2], who confirmed the recurrent behavior for quartic and cubic nonlinearity, called the superperiod of the FPU system. This recurrence was later understood as a consequence of the linear independence of the linear frequencies, and the superperiod was theoretically calculated using perturbation theory[3, 4]. The first theoretical prediction of a threshold to equipartition was obtained by Izraelev and Chirikov[5] using an overlap criterion for the fastest resonances. They predicted a critical energy of the initial excitation for widespread stochasticity. Subsequently there have been many studies of the interchange of energy among modes, and thresholds to give approximate equipartition among modes[6, 7, 8]. In particular Pettini and Landolfi[8] have studied the dependence of the relaxation time on the energy of the excitation. We note here that equipartition is related to the time one waits, for example the equipartition predicted in [5] should happen on a time scale of the order of the inverse of the smallest linear frequency, which is a time proportional to  $N$ , the number of particles in the FPU chain.

The usual numerical experiment on the FPU consists of distributing all the energy among some few of the lowest frequency linear modes and waiting

for it to spread. If the nonlinear terms are small enough then the energy shell is a hypersphere and ergodicity over the energy shell implies equipartition of energy among the linear modes, a well known result of microcanonical statistical mechanics. Equipartition is usually taken as a numerical test for ergodicity, even though it doesn't imply it.

A useful approximation to study the FPU Hamiltonian is the Birkhoff normal form perturbation theory[9]. Using normal forms a canonical transformation to new variables is made in which the quartic couplings between the linear modes can be removed and put into the next order, divided by a denominator in which frequency differences between modes appear. At small enough energies these frequency differences are sufficiently large, except in small regions of the phase space, that the ordering is preserved. As one raises the energy the most important nonlinear couplings of neighboring modes with the smallest frequency differences in the denominator can become resonant. We call these the "major resonances". At moderate energies it is useful to remove all the other terms and leave only the major resonances, obtaining the so called resonant normal form. In section 2 we introduce the FPU Hamiltonian, classify its quartic resonances and develop a theory for overlap of these major resonances. In section 3 we show numerical results on the FPU, and in section 4 we study the deformation of the linear modes and the coupling to the high-frequency modes.

## 2 Nonlinear Couplings and Resonances

The FPU Hamiltonian, representing a linear chain of equal masses coupled by nonlinear springs is

$$H = \left\{ \sum_{i=1}^N \frac{1}{2} p_i^2 + \frac{1}{2} (q_{i+1} - q_i)^2 + \frac{1}{4} \beta (q_{i+1} - q_i)^4 \right\}. \quad (1)$$

We consider only the case of fixed boundaries  $q_0 = q_{N+1} = 0$ . In the linear case ( $\beta = 0$ ) the chain of oscillators may be put in the form of  $N$  independent normal modes, and is therefore integrable and non-ergodic. Those normal modes are [3, 5] :

$$q_i = \sqrt{\frac{2}{1+N}} \sum_{\alpha=1}^N \sin(ki\alpha) \frac{1}{\sqrt{\Omega_\alpha}} Q_\alpha \quad i = 1, \dots, N \quad (2a)$$

$$\Omega_\alpha = 2 \sin\left(\frac{1}{2} k\alpha\right) \quad (2b)$$

$$k \equiv \pi/(N+1), \quad (2c)$$

where  $\Omega_\alpha$  is the frequency of the  $\alpha$ th linear mode and  $Q_\alpha$  its amplitude. We transform to these normal mode coordinates using a canonical transformation with generating function

$$F = \sqrt{\frac{2}{1+N}} \sum_{i,r=1}^N \sqrt{\Omega_\alpha} \sin(kir) q_i P_r. \quad (3)$$

so that the old momenta are given by

$$\begin{aligned} p_i &= \partial F / \partial q_i \\ &= \sqrt{\frac{2}{1+N}} \sum_{r=1}^N \sin(kir) \sqrt{\Omega_r} P_r. \end{aligned} \quad (4)$$

For algebraic convenience we will also use complex canonical coordinates defined by

$$Z_j \equiv \frac{1}{2} \sqrt{2i} (Q_j + iP_j)$$



$$Z_{-j} \equiv -\frac{1}{2}\sqrt{2i}(Q_j - iP_j), \quad (5)$$

where  $Z_{-j}$  is the variable canonically conjugate to  $Z_j$ , and as the  $P$ 's and  $Q$ 's are real at all times it can be seen from (5) that  $Z_j$  is the complex conjugate of  $iZ_{-j}$ . The Hamiltonian in these complex coordinates is[10]

$$H = \sum_{l=1}^N i\Omega_l Z_l Z_{-l} - c \sum_{r,s,m,n} G(r,s,m,n) Z_r Z_s Z_m Z_n, \quad (6)$$

where the indices in the last sum run from  $-N$  to  $N$ , zero excluded,  $c \equiv \frac{\beta}{2^5(N+1)}$  and the coupling strength  $G$  is

$$G(r,s,n,m) \equiv \lambda_r \lambda_s \lambda_n \lambda_m \sum_P B(r+s+n+m), \quad (7)$$

where  $\lambda_\alpha \equiv \text{sign}(\alpha)\sqrt{\Omega_{|\alpha|}}$ , and  $B$  is defined by

$$B(\alpha) = \begin{cases} 1 & \text{if } \alpha = 0 \\ -1 & \text{if } \alpha = \pm 2(N+1) \\ 0 & \text{otherwise} \end{cases}, \quad (8)$$

and  $\sum_P$  in (7) represents the sum over all the eight permutations of sign of  $s, n, m$ . The quartic term brings nonlinear corrections to the frequency as well as quartic couplings. According to the harmonic part of (6) the amplitudes  $Z_\alpha$  evolve like  $\exp(i\Omega_\alpha t)$  and the amplitudes  $Z_{-\alpha}$  of negative index evolve with a negative frequency like  $\exp(-i\Omega_\alpha t)$ . In this way we can generalize equation (2b) to negative index and then the amplitudes  $Z_\alpha$  have frequency  $\Omega_\alpha$  for  $\alpha$  negative or positive.

The quartic term is a sum of products of four amplitudes with indices respecting some selection rules (7). We designate the indices are  $r, s, m, n$ . The frequency of this monomial is  $\Delta\Omega = \Omega_r + \Omega_s + \Omega_m + \Omega_n$ . Now assume all these indices are small enough that the dispersion relation can be approximated by its linear part plus cubic correction. Expanding  $\Delta\Omega$  in powers of

$k$  using (2) we obtain

$$\begin{aligned}\Delta\Omega &= \frac{1}{2}k(r+s+m+n) \\ &+ \frac{1}{48}k^3(r^3+s^3+m^3+n^3) + O(k^5).\end{aligned}\quad (9)$$

Because we want the smallest values of  $\Delta\Omega$  we see that we can make the first order in  $k$  equal to zero by setting  $r+s+n+m=0$  and this also automatically makes these four indices satisfy the selection rule(7). Eliminating the index  $r = -s - m - n$  from  $\Delta\Omega$  we obtain

$$\Delta\Omega = \frac{1}{8}k^3(m+n)(s+m)(s+n) + O(k^5).\quad (10)$$

For fixed  $m, n$  this is a parabola in  $s$  with minimum at  $s = -\frac{1}{2}(m+n)$  and minimum value  $\Delta\Omega = \frac{1}{4}k^3ri^2$ , where  $i \equiv \frac{1}{2}(m-n)$ . We call this resonance involving modes  $r, r+i$ , and  $r-i$  a major resonance. Because  $\Delta\Omega$  is proportional to  $i^2$  we limit ourselves to the resonances where  $i = 1$  as they are more important at small energies. We will explore the approximation in which the nonlinear coupling at moderate energies can be expressed by a resonant normal form containing only these major resonances.

It is well known that the new actions for the coupled problem have only an asymptotic expansion due to the presence of the resonances. Because the perturbation is a quadratic function of the energy, the deformation of the actions is a monotonic function of the energy. One has to be careful to separate this deformation from diffusion due to nonintegrability.

We now construct an order parameter for nonlinear deformation of the actions, which can be related to the formation of resonances. The parameter is also related to overlap of these islands and accompanying stochasticity. We want to understand the situation where the excitation involves only a few

modes and therefore study the case where only two resonances are important. As we will see, systems with only two primary resonances can easily be studied numerically by the method of surface of section. One major resonance involves three consecutive modes and since we want two resonances it is natural to pick four consecutive modes as our model. We will call this subsystem the 1234 system. Assuming that the energy stays in those four modes and all the other modes have ignorable amplitude we then study the four degree of freedom system obtained by putting all the other coordinates equal to zero in the FPU Hamiltonian (6) [11]. We can transform the Hamiltonian in (6) back to the real  $P$  and  $Q$  coordinates using (5) so that the Hamiltonian for the subsystem is

$$\begin{aligned}
H = & \sum_1^4 \frac{1}{2} \Omega_i (P_i^2 + Q_i^2) \\
& + \frac{d}{4} [\sum_1^4 \Omega_i^2 Q_i^4 + \sum_{i>j} 4\Omega_i \Omega_j Q_i^2 Q_j^2] \\
& + d\sqrt{\Omega_1 \Omega_2^2 \Omega_3} Q_1 Q_2^2 Q_3 + d\sqrt{\Omega_2 \Omega_3^2 \Omega_4} Q_2 Q_3^2 Q_4 \\
& + 2d\sqrt{\Omega_1 \Omega_2 \Omega_3 \Omega_4} Q_1 Q_2 Q_3 Q_4.
\end{aligned} \tag{11}$$

In the above equation  $d$  is defined as  $d \equiv \frac{3\beta}{2N+2}$ . We have used the real  $P$ 's and  $Q$ 's for convenience of the numerical integration algorithm. The frequencies are the first four consecutive frequencies in the low wavelength part of the dispersion relation, where the frequency can be approximated by expansion up to cubic order in powers of  $k$ . This can be generalized to any set of four consecutive modes  $\alpha + 1, \alpha + 2, \alpha + 3, \alpha + 4$  where  $\alpha$  is any positive integer small compared to  $N$ . The frequencies are then renamed as

$$\Omega_i = 2 \sin\left(\frac{1}{2}k(i + \alpha)\right), \quad i = 1, \dots, 4 \tag{12}$$

and  $Q_i$  stands for the coordinate of mode  $\alpha + i$ . The two slow angles of the major resonances are  $\theta_s = \theta_1 + \theta_3 - 2\theta_2$  and  $\theta_{sp} = \theta_2 + \theta_4 - 2\theta_3$ , where  $\theta_i$ ,  $i = 1, \dots, 4$  is the angle of  $i$ th oscillator of the subsystem(11), which comes from the  $(i + \alpha)$ th mode of the FPU chain. We refer to the appendix where we use normal forms to remove all the fast nonlinear angle dependent terms except the ones that depend on  $\theta_s$  and  $\theta_{sp}$ . We are left with two adiabatic constants of motion plus two coupled degrees of freedom, with slow angles  $\theta_s$  and  $\theta_{sp}$ , that can be studied numerically in a surface of section. In the following we will also study an approximation to this Hamiltonian as a means to understand the deformation of the slow actions.

The canonical transformation to slow actions is accomplished by the generating function

$$F = J_s(\theta_1 + \theta_3 - 2\theta_2) + J_{sp}(\theta_2 + \theta_4 - 2\theta_3) + J_c\theta_3 + J_d\theta_4. \quad (13)$$

The explicit transformations of the actions are:

$$\begin{aligned} J_1 &= J_s \\ J_2 &= J_{sp} - 2J_s \\ J_3 &= J_s - 2J_{sp} + J_c \\ J_4 &= J_{sp} + J_d. \end{aligned} \quad (14)$$

The actions on the left sides of (14) have to be positive, which imposes a domain for the values of  $J_{sp}$  and  $J_s$ , represented by the shaded area in figure 1. The adiabatic constant  $J_c$  is a positive function of the original actions given by

$$J_c = 3J_1 + 2J_2 + J_3. \quad (15)$$

The actions  $J_s$  and  $J_{sp}$  are conjugate to the two slow angles  $\theta_s$  and  $\theta_{sp}$  and  $J_c$  and  $J_d$  are conjugate to the angles  $\theta_3$  and  $\theta_4$  respectively. In the appendix we use a normal form expansion to obtain the Hamiltonian in terms of the slow variables. If we divide the Hamiltonian (A10) by  $\frac{1}{4}(3 + \alpha)k^3J_c$  and scale the slow actions to  $J_c$ , the resulting Hamiltonian depends only on a single parameter  $R$ . This parameter, measuring the quotient of the quadratic energy of the slow actions to the linear energy of the slow actions, is

$$R \equiv 4d(3 + \alpha)kJ_c/k^2. \quad (16)$$

$R$  is an order parameter for the size of the first order correction to the slow frequencies. Note that  $R$  depends on  $\alpha$  only via the combination  $(3 + \alpha)kJ_c$  which is the initial linear energy. The quantity  $R$  is proportional to  $N$  times the initial linear energy put in mode  $(3 + \alpha)$ .

We now develop an approximation to the motion under this Hamiltonian. We observe numerically that the two slow angles drift with almost the same speed in most of the energy shells. As an approximation to calculate the beats of the two slow angles we assume that the slow angle  $\theta_{sp}$  drifts at a constant speed  $\omega$  and that the angle  $\theta_s$  moves by  $\theta_s = \omega t + \theta_b$ , where  $\theta_b$  is the beat angle.

We now make a canonical change from the slow angle  $\theta_s$  to the beat angle  $\theta_b$ , which adds the linear term  $-\omega J_s$  to the Hamiltonian (A10). The action conjugate to the beat angle is still  $J_s$ . Although the orbit of  $\theta_{sp}$  is a near-constant drift at speed  $\omega$ , the slow action  $J_{sp}$  oscillates with frequency  $\omega$  and amplitude  $\mu J_c$  around some value  $J_{spo}$ , ( $J_{sp} = J_{spo} + \mu J_c \cos(\omega t)$ ). The numerical value for  $\omega$  is  $\omega \sim 0.6\gamma Rk^3$  for most orbits in the energy shells of figure 2. Substituting this assumed orbit into the Hamiltonian (A10) we obtain a time dependent Hamiltonian for  $J_s$  and  $\theta_s$ , which we average over

time to obtain a pendulum Hamiltonian for the beat angle  $\theta_b$

$$H_s = -[0.25 + R(0.5 - 4J_{spo})]\gamma k^3 J_s + \frac{3}{8}R\gamma k^3 J_s^2 - \frac{1}{16}\mu\gamma Rk^3 J_c^2 \cos(\theta_b). \quad (17)$$

In the above equation  $\gamma$  is defined as  $\gamma \equiv (3 + \alpha)$  with  $\alpha$  defined in (12). To obtain the term in  $\cos(\theta_b)$  we have expanded the Hamiltonian (A10) to first order in  $\mu$  and averaged the time dependence away. The result still depends on  $J_{spo}$  and  $J_s$  and we substituted it by a typical value. The minimum value of  $R$  for the appearance of a fixed point of  $J_s$  for the Hamiltonian  $H_s$  of (17) in the allowed range of the actions is  $R = 0.33$ . Numerically, the surface of section of the Hamiltonian (49), shown in figure 2, indicates that the fixed point appears at  $R \sim 0.5$ .

The constant  $\mu$  depends on the oscillatory term of  $J_{sp}$  and requires knowledge of the orbit. We calculate it numerically from the frequency of the beat angle  $\theta_b$  at the center of the island

$$\Omega_b = 0.2\gamma Rk^3 \quad (18)$$

and  $\mu$  is calculated to be 0.85. We choose an initial condition  $J_s = 0.055J_c$ ,  $J_{sp} = 0.527J_c$  and  $\theta_s = \theta_{sp} = 0$  which defines an energy shell for a given  $R$ . In the numerical integration of (A10) we used  $N = 256$  and  $\alpha = 36$ . We start several initial conditions on this energy shell and plot  $J_s$  versus  $\theta_s$  in a surface of section at  $\theta_{sp} = 0$  for  $R = 0.5$ ,  $R = 1.5$ ,  $R = 4.5$  and  $R = 10.0$ . We normalize all the actions to  $J_c$  so that  $J_c$  can be taken to be one. From figure 1 we see that  $J_s$  can vary from zero to  $0.33J_c$ . In figure 2 for the energy shell at  $R=0.5$  the slow action is nearly constant for most of the phase space, and the first resonance island has just been born. We

call this the near-linear regime. Above  $R = 0.5$  the topological change in the surface of section, which has taken place, grows in importance. These islands are the well known superperiods of the FPU chain[2]. At  $R = 1.5$  there are two islands present but no noticeable stochasticity. At  $R = 4.5$  and above there is considerable stochasticity. Increasing the energy in the normal form of the 1234 system above  $R = 10.0$  does not significantly change the phase space since the quartic terms in the Hamiltonian[see Appendix, Eq(A10)]dominate over the quadratic part such that the parameter  $R$  factors out of the Hamiltonian. In this parameter range, the frequency of the motion around a fixed point is proportional to  $(3 + \alpha)Rk^3$  as in (18). In the FPU Hamiltonian the energy can leave the 1234 system, as there is coupling to all the other modes. As the energy is increased more modes will be involved in a significant way, but we assume that as long as the energy is concentrated in a small number of modes around mode  $3 + \alpha$ , the characteristic frequency for the beats of the slow angles of low frequency modes will still be proportional to  $(3 + \alpha)Rk^3$  as in (18).

### 3 Numerical Results for the FPU System

We discuss some numerical calculations performed on the FPU system. We use initial conditions for which all the energy is concentrated in some few modes around some mode  $\gamma = 3 + \alpha$ . We use two different initial conditions here called A and B. Initial condition A corresponds to  $J_d = 0$ ,  $J_s = 0.0315J_c$  and  $J_{sp} = 0.066J_c$  in the 1234 model. Initial condition B corresponds to  $J_d = 0$ ,  $J_s = 0.083J_c$  and  $J_{sp} = 0.457J_c$ . The energies of all the other modes but modes  $i + \alpha$ ,  $i = 1, \dots, 4$  are all set to zero. Initial condition A has most of the energy (91%) in mode  $3 + \alpha$ , and the energy shells of figure 2 were

defined by the energy of initial condition B. Also we take  $\beta$  equal to 0.1, as was done by other authors [6, 7, 8]; this value can always be rescaled to any positive finite number by a linear rescaling of the distances in the FPU chain. The numerical integrations are performed on a supercomputer CRAY C90 using a fourth order symplectic integration algorithm[13]. The error in the energy was monitored to be less than one part in a thousand for all the runs.

As we remarked in section 2, for small values of  $R$  the nonlinear deformation is small and will involve only some few modes. For an FPU system with many degrees of freedom, if the initial energy is in mode  $\gamma$  we might expect it to couple successively to the nearby modes until the “local” value of  $R$  is less than 0.5. By this reasoning we should expect that the number of modes excited by the nonlinear deformation should be proportional to  $R$ . At the energies we are studying the quartic part of the full FPU Hamiltonian is  $k^2$  times smaller than the harmonic part so that the functional form of the Hamiltonian is effectively harmonic. Because of this, if the system is ergodic on the energy shell, then the linear mode energies should all have nearly the same time average. In our numerical experiments we always calculate the time average of the linear energies, here referred to as  $E_i$ ,  $i = 1, \dots, N$ .

We introduce the information entropy[7, 14, 15]

$$S = \ln\left(\sum_{i=1}^N E_i\right) - \sum_{i=1}^N E_i \ln E_i, \quad (19)$$

and define the effective number of modes by

$$n_{ef} \equiv \exp(S). \quad (20)$$

If the motion is ergodic on the time scale considered then  $n_{ef}$  will be equal to  $N$ . As we saw in (18), for large enough  $R$  the characteristic frequency of



oscillation for the amplitude of the low frequency modes is  $0.2\gamma Rk^3$ , which can be written as  $0.65\gamma k^2 R/(N+1)$ . As we will see later, there is another important frequency related to the resonance of the high frequency modes which is proportional to  $\gamma k^2$ . Then, for fixed  $R/(N+1)$ , the only frequency scale in the system is  $\gamma k^2$ . Therefore we chose the natural time scale to plot the solutions for the integrations of the FPU at fixed values of  $R/(1+N)$  (figures 4,5,6) to be  $3/\gamma k^2$ . (The 3 was chosen such that for the lowest value of  $\gamma = 3$  the time scale is  $1/k^2$ .) In the following numerical experiments we integrate the system for times up to 208000 times  $3/\gamma k^2$ . In figure 3 we show a histogram of the average mode energy over a time of  $4000(3/\gamma k^2)$  starting with energy corresponding to  $R = 2.9$  in mode 3. We can see from figure 3 that the energy stays mostly in mode 3 and its immediate neighbors. The value of  $n_{ef}$  from (20) is 3.26. If we start with larger values of  $R/(N+1)$ , the number of modes found to share the energy is proportionately larger. In figure 4, using initial condition A, we plot the effective number of modes versus scaled time for three values of  $R$ . There appears to be a transition near  $R/(N+1) \approx 0.2$  such that for smaller values the spreading among modes will saturate, while for larger values the system evolves to near-equipartition. We also use the initial conditions around mode  $3 + \alpha$  with nonzero integer  $\alpha$  and find that the evolution of  $n_{ef}$  as a function of scaled time is independent of  $\alpha$  for  $\alpha$  small compared to  $N$ . The solid curve in figure 4, for the case of  $\gamma = 3 + \alpha = 6$  lies on the curve with the same  $R$  and  $\gamma = 3$ . With the two different initial conditions the results were quantitatively similar, showing the formation of a plateau for  $R/(N+1)$  below 0.17 while above this value evolution to near-equipartition occurs. In all numerical experiments we observed that the number of modes evolved from one at  $t = 0$  to a constant final value in times of less than  $100(3/\gamma k^2)$ , for values of  $R/(N+1)$

for which saturation occurs. This suggests that these low frequency modes close to the mode in which most of the energy is placed obtain energy by deformation rather than diffusion to the final steady plateau. In figure 5 we repeat the results for the same values of  $R/(N + 1)$  and initial condition A but for  $N = 64$ . We observe that the transition values are quite similar, indicating that  $R/(N + 1)$  is the controlling parameter. Note also that the value of  $(n_{ef} - 1)/N$  obtained at a given normalized time, for a given value of  $R/(N + 1)$  above the transition, is approximately the same for  $N = 32$  and  $N = 64$ . In figure 6 we have plotted  $(n_{ef} - 1)/N$  versus normalized time for  $N = 16$ ,  $N = 32$ ,  $N = 64$  and  $N = 128$ . We observe that all the points stay close to a universal curve.

In figure 7 we plot the height of the plateau versus  $R$  for different  $N$  values and initial condition A, after a time of  $t = 2000(3/\gamma k^2)$ . We observe that for a given  $N$  the value of  $n_{ef}$  in the plateau is proportional to  $R$  up to a critical value  $R_c$ . This value  $R_c$  is found numerically to be proportional to  $N$ . We see in the figure that for  $N = 16$  it is 2.9 and for  $N = 32$  it is 5.8. For  $N = 64$  the transition occurs at  $R_c = 11.6$  (see figure 5). For all of these values we find the transition at  $R_c/(N + 1) = 0.17$ . For values of  $R$  larger than  $R_c$  the number of modes appears to evolve towards near-equipartition.

In figures 8 and 9 we show the average mode energy on a logarithmic scale for two different values of  $R$ . The average linear energies were normalized so that the total average linear energy is one. We see that for  $R = 2.9$  and  $N = 32$  the initially zero energies of the high frequency modes, which rapidly evolve to values near or below  $\exp(-10)$ , are found to remain at these low values for much longer times. At  $R = 8.0$  and  $N = 32$  some high frequency modes acquire a much larger energy of order  $\exp(-5)$  in a relatively short time, and continue to increase in energy, with energy being transferred to other

modes on a longer time scale. We can observe this longer time approach to near-equipartition at  $R = 8.0$  and  $N = 32$  in figure 10. This process of transferring energy selectively to certain high-frequency modes is treated in the following section.

## 4 Coupling and Diffusion to High Frequency Modes

The initial energy in a low frequency linear mode will spread to all the other linear modes via the quartic coupling. We assume that most of the energy is initially in mode  $\gamma \equiv 3 + \alpha$  with all other modes having much smaller energies. We also note that the linear mode  $\gamma$  is not an exact mode of the nonlinear system because it is coupled to all the other linear modes. The selection rule for the coupling in Hamiltonian (6) requires that permutations of the signs of the four mode indexes must add to zero for the term to be present in the quartic coupling. In the approximation that all the energy is in the linear mode  $\gamma$  the only coupling for the high-frequency mode  $h$  is to modes  $h \pm 2\gamma$  to first order in  $|Z_\gamma|^2$ . The major resonance coupling treated in section 2 is important only for the interaction of a few neighboring low-frequency modes. In the approximation that most of the energy is in some low-frequency mode the dominant nonlinear interaction with high-frequencies is via a quartic coupling involving two high-frequency modes and the low-frequency mode  $\gamma$  which contains most of the energy. Inspecting the quartic part of Hamiltonian (6) we find that the high-frequency mode  $h$  is coupled to modes  $h - 2\gamma$  and  $h + 2\gamma$  via

$$H_4 \simeq \sum_h 24ic\Omega_\gamma\Omega_h|Z_\gamma|^2 Z_{-h}(Z_{h-2\gamma} + Z_{h+2\gamma}). \quad (21)$$

where we have approximated the frequencies of modes  $h - 2\gamma$  and  $h + 2\gamma$  in (21) by  $\Omega_h$ , the frequency of mode  $h$ . There is a coupling of the same type from mode  $h$  to itself but it only changes the frequency of the modes by a fixed small amount and we have omitted it. Considering  $Z_\gamma$  in (21) to be constant, then (21) is a quadratic coupling among the linear high-frequency modes. We then rediagonalize the Hamiltonian to obtain the new normal modes, by using normal forms[9]. The coupling is removed in fourth order by a canonical transformation with generating function[9]

$$F_4 = \sum_h z_h Z_{-h} + b_h |Z_\gamma|^2 Z_{-h} (z_{h-2\gamma} + z_{h+2\gamma}). \quad (22)$$

The coefficient  $b_h$  is obtained by the condition that the term  $H_4$  of (21) is canceled from the quartic order by the quasi-identity canonical transformation. The coefficient  $b_h |Z_\gamma|^2$  is found to be

$$b_h = -24c\Omega_\gamma\Omega_h/(\Omega_{h+2\gamma} - \Omega_h). \quad (23)$$

Because the new coordinates  $z_h$  are uncoupled to quartic order it turns out that their amplitudes  $|z_h|$  are constant over times of order  $2\pi/(\Omega_{h+2\gamma} - \Omega_h) \approx 2\pi/\gamma k^2$  in the case that  $b_h$  is small. The old coordinate  $Z_h$  is defined by

$$\begin{aligned} Z_h &= \partial F_4 / \partial Z_{-h} \\ &= z_h + b_h |Z_\gamma|^2 (z_{h-2\gamma} + z_{h+2\gamma}). \end{aligned} \quad (24)$$

At  $t = 0$  the value of the old coordinate  $Z_h$  is zero unless  $h = \gamma$ , in which case it is equal to the initial amplitude  $Z_\gamma$ . If we assume  $b_h |Z_\gamma|^2$  to be small it can be seen from (24) that the new coordinate  $z_\gamma$  at  $t = 0$  is approximately equal to  $Z_\gamma$ . We use this value of  $z_\gamma$  and (24) with  $h = 2\gamma$  to obtain the value of  $z_{2\gamma} \simeq b_{2\gamma} |Z_\gamma|^2 Z_\gamma$ . In this way we solve for all the amplitudes  $z_\gamma, z_{3\gamma},$

$z_{5\gamma}, \dots$  which are found to decay geometrically according to

$$z_h = \rho_h z_{h-2\gamma}, \quad (25)$$

where  $\rho_h$  is given by

$$\rho_h = |b_h| J_c, \quad (26)$$

and  $J_c = |Z_\gamma|^2$  is the action of mode  $\gamma$ , assumed to contain almost all of the energy. Thus if we put the initial energy in mode 3 ( $\gamma = 3$ ) the amplitude  $z_9$  is a small factor  $\rho_3$  times  $z_3$  and then another small factor  $\rho_9$  for  $z_{15}$  and so on. Because the factors are not all the same, we evaluate the average factor  $\rho$  defined by

$$\rho^{N/2\gamma} = \rho_\gamma \rho_{3\gamma} \dots \rho_{N-2\gamma}, \quad (27)$$

approximated for large  $N$ . We now eliminate  $J_c$  in favor of  $R$  using (17) and substitute (23) into (26), with the frequency  $\Omega_h$  given by (2a), to obtain the formula for the factor of index  $h$

$$\rho_h \approx \left(\frac{kR}{4\gamma}\right) \tan\left(\frac{k(2h + \gamma)}{4}\right) \quad (28)$$

The average logarithm of the tangent with  $h$  running from 1 to  $N$  is zero, so the average factor is

$$\rho = \left(\frac{\pi R}{4\gamma(N + 1)}\right). \quad (29)$$

This approximation is valid for the assumption that all the high-frequency modes have a much smaller amplitude than mode  $\gamma$ , and so it is valid only if the factor  $\rho$  is much smaller than one, that is, if  $R/(N + 1)$  is small. Now within the approximation that the amplitudes  $z_h$  have a constant modulus

and according to (24) and (25) the average linear energies  $\Omega_h|Z_h|^2$  will also decay in a geometric progression

$$E_h \simeq \rho^2 E_{h-2\gamma}. \quad (30)$$

In figure 11 we plot the natural log of the average energies for two values of  $\gamma$ . We see that mode  $h$  is mainly coupled to mode  $h - 2\gamma$  because the mode energies show an exponential decrease superposed to an oscillation of period  $2\gamma$ . The solid line in figure 11 is the geometric progression calculated from (30) and (29); the crosses are the numerical calculations. Due to machine round-off the average mode energies after mode 32 are all given by  $\exp(-26)$ . In figure 11 the equations of motion were integrated for a short time of the order of  $\Omega_N - \Omega_{N-2\gamma} \sim \gamma k^2$ . This is in contrast with figures 8 and 9 in which the integration was over a much longer time, such that the oscillation of period  $2\gamma$  in the mode energies was washed away. In figure 9, a larger value of  $R/(N+1)$  was used so that the asymptotic approximation (29) does not hold.

For larger  $R/(N+1)$ , where the above approximation does not hold, we must use another method to calculate the effect of the coupling (21). In the following we provide an estimate of the effect of terms of type (21) on the coupling to high-frequency modes for large  $R/(N+1)$  where from section 2, we expect stochastic interaction among neighboring low-frequency modes. We make the following assumptions regarding the orbit of the low frequency modes: We use the approximation of section 2 and assume that the dynamics of the beat angle is in a stochastic region; we also assume the trajectory is sufficiently close to a separatrix that the separatrix equation for the Hamiltonian (17)

$$\theta_{sx} = 4 \arctan(e^{\Omega_b t}) - \pi \quad (31)$$

$$J_s = J_{so} + 4J_c(\mu/24)^{1/2} \cos\left(\frac{\theta_{sx}}{2}\right), \quad (32)$$

describes the motion. Here  $J_c$  is the constant action defined in equation (12) and  $\mu$  is defined below (17). Substituting this separatrix orbit of  $J_s$  and the periodic orbit of  $J_{sp}$ , assumed in (17), into (14), we find the variation of  $J_3$ . Setting  $|Z_\gamma|^2 = J_3$  we obtain

$$\begin{aligned} |Z_\gamma^2| &= J_c + J_{so} - 2J_{spo} - 2\mu J_c \cos(\omega t) \\ &\quad + 4J_c\left(\frac{\mu/24}{3}\right)^{1/2} \cos\left(\frac{\theta_{sx}}{2}\right). \end{aligned} \quad (33)$$

We then consider the term  $H_4$  of (21) plus the linear part of (6) to obtain the equation of motion for  $Z_h$ ,

$$\frac{dZ_h}{dt} = i\Omega_h Z_h + 24ic\Omega_\gamma\Omega_h |Z_\gamma|^2 (Z_{h-2\gamma} + Z_{h+2\gamma}). \quad (34)$$

We introduce slow variables  $Y_h(t)$  by

$$Z_h(t) = e^{i\Omega_h t} Y_h(t), \quad (35)$$

and substitute (33) and (35) in (34) to obtain the differential equation for  $Y_h$

$$\frac{dY_h}{dt} \simeq c_- Y_{h-2\gamma} + c_+ Y_{h+2\gamma}, \quad (36)$$

where

$$\begin{aligned} c_- &\equiv 24ic\Omega_h\Omega_\gamma (J_c - 2J_{spo} - 2\mu J_c \cos(\omega t)) e^{i\Delta\Omega_h t} \\ &\quad + 96ic\Omega_h\Omega_\gamma J_c \left(\frac{\mu}{24}\right)^{1/2} e^{i\Delta\Omega t} \cos(\theta_{sx}/2) \end{aligned} \quad (37)$$

and  $\Delta\Omega_h \equiv (\Omega_{h-2\gamma} - \Omega_h)$ . Assuming that the amplitudes  $Y_{h-2\gamma}$  and  $Y_{h+2\gamma}$  stay constant going around the separatrix, the kick  $\Delta Y_h$  is calculated by integrating (36) over the separatrix orbit, with the leading term

$$\Delta Y_h = \Delta c_{-2\gamma} Y_{h-2\gamma}, \quad (38)$$

where  $\Delta c_-$  is given by

$$\Delta c_- \equiv 96ic\Omega_h\Omega_\gamma J_c\left(\frac{\mu}{24}\right)^{1/2} \int_{-\infty}^{\infty} \cos\left(\frac{\theta_{sz}}{2}\right) e^{-i\Delta\Omega_h t} dt \quad (39)$$

The integral is an Melnikov-Arnold integral described by Chirikov[12] which when evaluated in (39) gives

$$\Delta c_- = \frac{4\pi i}{0.9\gamma k} \left(\frac{3\mu}{8}\right)^{1/2} e^{-\pi\lambda_h/2}, \quad (40)$$

where

$$\lambda_h \equiv (\Omega_h - \Omega_{h-2\gamma})/\Omega_b \approx 1.59(N+1)(N+1-h)/R.$$

If we assume that the amplitudes  $Y_h$  were initially described by the geometric progression of (25) then

$$Y_h = \rho Y_{h-2\gamma}. \quad (41)$$

Substituting (41) and (40) with  $h = N$  into (38) the kick in  $Y_N$  can be written as

$$\frac{\Delta Y_N}{Y_N} = \frac{10.6}{k} \left(\frac{3\mu}{8}\right)^{1/2} (1/x) e^{-(1/x)}, \quad (42)$$

where  $x \equiv 0.4R/(N+1)$ . The functional form (42) obtained for the stochastic kick is exponentially small up to  $R/(N+1) \approx 0.25$  and then grows rapidly to order one above this value. The mechanism then is that random kicks are given to the high-frequency modes by their resonant interaction with the beat modes. The period of the kicks is that of the average beat motion in the stochastic region. This mechanism, known as Arnold diffusion, has been described by Chirikov[12]. According to the mechanism, energy is pumped into the high frequency modes above the critical value of  $R/(N+1) \approx 0.25$ .



This is verified computationally in figures 4, 5 and 6 which show similar behavior for the same values of  $R/(N + 1)$  with  $N = 32$  and  $64$ . The numerically determined critical value from figure 7 is  $R/(N + 1) = 0.17$ . The Arnold diffusion scaling close to the critical value is very hard to test numerically because of the very long computational times required. We have tested this exponential scaling for values above the critical value. For example one can see from figure 5 that for  $R = 17.2$  and  $N = 64$  the value  $(n_{ef} - 1)/N = 0.63$  is reached in a normalized time of 40000. For  $R = 11.6$  using an approximate exponential scaling with  $R$  at fixed  $N$ , a normalized time of  $40000 \exp(17.2/11.6) = 176000$  is predicted. Numerically, this time is found in figure 5 to be 208000.

## 5 Conclusion and Discussion

To gain further understanding about the route to equipartition by coupling to the high frequency modes we note that the frequency difference between the two high frequency modes of numbers  $N - j$  and  $N - j - 2\gamma$ , which are the ones that couple according to the selection rule, is

$$\Delta\Omega_h = \gamma k^2(1 + j), \quad (43)$$

which is a multiple of the fundamental frequency  $\Delta\Omega_o \equiv \gamma k^2$ . According to equation (18) the frequency of the beats of the low frequency modes for large enough  $R$  is  $\Omega_b = 0.2\gamma Rk^3$ . These two frequencies determine the two time scales in the route to equipartition. After a time  $t$  of integration, we might expect the number of modes excited to be given in the form

$$(n_{ef} - 1)/N = g(\Omega_b t, \Delta\Omega_o t), \quad (44)$$

It is therefore natural to expect the parameter controlling equipartition to be the ratio of the two time scales  $\Omega_b/\Delta\Omega_o \sim R/(1 + N)$  . This explains our finding that  $R_c$  is proportional to  $N + 1$  and is also in agreement with numerical results of Livi and Ruffo[16] that equipartition is reached at a fixed energy independent of  $N$ . [ $R/(N+1)$  is the linear energy of the FPU system]. Also, for a fixed ratio  $\Omega_b/\Delta\Omega_o = 0.65R/(1 + N)$ ,  $(n_{ef} - 1)/N$  should be a universal function of  $\Delta\Omega_o t$ . This is in agreement with the computational results which can be seen in figure 6 where we plotted  $(n_{ef} - 1)/N$  versus  $\gamma k^2 t$  for  $R/(N + 1) = 0.25$  and  $N=16, 32, 64$  and  $128$ .

Our results indicate a transition where, above a critical energy, equipartition can be reached if one waits for a time of the order of  $3/\gamma k^2$  . Below this critical energy the time will be exponentially long. The critical energy for equipartition was found to be independent of the low-frequency mode  $\gamma$  used as an initial condition. This is consistent with having ergodicity on the energy shell as it then should not matter what initial conditions are chosen.

The exponentially long time scale for interchange of energy between resonances with well separated frequencies does not depend on the special assumptions we have made here; it was shown by Benettin, Galgani and Giogilli[17] that one can decouple a set of fast oscillators, in our case the high-frequency modes, from a mechanical system with slower frequency, here  $0.65\gamma Rk^2/(N + 1)$  as seen in (18). By using a set of canonical transforms one can reduce the coupling to the fast oscillators to a size exponentially small in the ratio of the frequencies. This is in agreement with the result we obtained using the approximation of driving motion in a separatrix layer.

## Appendix: Normal forms

In this appendix we show how to remove the fast angles from the 1234 Hamiltonian (11) with the use of normal forms[9]. First we go back to the complex coordinates of (5)

$$\begin{aligned} Z_j &\equiv \frac{1}{2}\sqrt{2i}(Q_j + iP_j) \\ Z_{-j} &\equiv -\frac{1}{2}\sqrt{2i}(Q_j - iP_j), \end{aligned} \quad (\text{A1})$$

where  $i$  is the square root of minus one and  $j = 1, \dots, 4$ . This is a canonical transformation with inverse

$$\begin{aligned} P_j &= \sqrt{i/2}(Z_j + Z_{-j}) \\ Q_j &= (Z_j - Z_{-j})/\sqrt{2i}. \end{aligned} \quad (\text{A2})$$

Substituting those complex variables into the Hamiltonian( 11) we get a harmonic part plus a quartic polynomial

$$H = \sum_{l=1}^4 i\Omega_l Z_l Z_{-l} + \text{quartic polynomial} \quad (\text{A3})$$

To remove fast terms from the quartic polynomial a canonical transformation to new variables  $z_{-j}$  and  $z_j$  is performed using a generating function  $S_4$

$$\begin{aligned} Z_{-j} &= z_{-j} + \partial S_4 / \partial Z_j \\ z_j &= Z_j + \partial S_4 / \partial z_{-j}. \end{aligned} \quad (\text{A4})$$

For example if we want to remove a generic quartic monomial like  $t4 = cZ_1^{\alpha_1} Z_2^{\alpha_2} Z_3^{\alpha_3} Z_4^{\alpha_4} Z_{-1}^{\beta_1} Z_{-2}^{\beta_2} Z_{-3}^{\beta_3} Z_{-4}^{\beta_4}$  then we use the generating function  $S_4 = -i(t4)/\Delta\Omega$  where  $\Delta\Omega$  is defined by :

$$\Delta\Omega = (\alpha_1 - \beta_1)\Omega_1 + (\alpha_2 - \beta_2)\Omega_2 + (\alpha_3 - \beta_3)\Omega_3 + (\alpha_4 - \beta_4)\Omega_4. \quad (\text{A5})$$

The Hamiltonian in the new variables cancels the quartic polynomial  $t_4$ , retaining the same linear part plus a sixth order term, and we say the quartic term has been “removed”. This procedure can be carried only if  $\Delta\Omega$  is nonzero.

It can also be seen that for this canonical transformation to be a quasi-identity transformation,  $\Delta\Omega$  must be larger than the maximum absolute value of  $t_4$ . Because of this, when the value of  $t_4$  is of  $O(k^3)$  we can safely remove all the monomials where  $\Delta\Omega$  is of  $O(k)$ . For example the coupling term  $Q_1Q_2Q_3Q_4$  when written in terms of the  $Z$ 's is

$$Q_1Q_2Q_3Q_4 = \left(\frac{1}{2i}\right)^2(Z_1 - Z_{-1})(Z_2 - Z_{-2})(Z_3 - Z_{-3})(Z_4 - Z_{-4}). \quad (\text{A6})$$

It can be found by inspection that the only monomial in the above equation that has  $\Delta\Omega$  of order  $O(k^3)$  is

$$t_{1234} = \left(\frac{1}{2i}\right)^2(Z_1Z_4Z_{-2}Z_{-3} + Z_{-1}Z_{-4}Z_2Z_3). \quad (\text{A7})$$

which we call the normal form of the term. Analogously the normal form of the other terms can be found. The term  $Q_1Q_2^2Q_3$  has normal form :

$$t_{1223} = \left(\frac{1}{2i}\right)^2(Z_1Z_3Z_{-2}^2 + Z_{-1}Z_{-3}Z_2^2). \quad (\text{A8})$$

The normal form of the 1234 Hamiltonian (11) can be calculated to be

$$\begin{aligned} H_n = & \sum_{l=1}^4 \frac{1}{2} \Omega_l J_l + \frac{d}{4} \left[ \sum_{l=1}^4 \frac{3}{4} \Omega_l^2 A_l^2 + \sum_{l>s} \Omega_l \Omega_s J_l J_s \right] \\ & + \frac{d1}{8} t_{1234} + \frac{d2}{8} t_{1223} + \frac{d3}{8} t_{2334}. \end{aligned} \quad (\text{A9})$$

where  $d \equiv 3\beta/(2N + 2)$ ,  $d1 \equiv 2d\sqrt{\Omega_1\Omega_2\Omega_3\Omega_4}$ ,  $d2 \equiv d\sqrt{\Omega_1\Omega_2^2\Omega_3}$ ,  $d3 \equiv d\sqrt{\Omega_2\Omega_3^2\Omega_4}$  and  $J_k \equiv (P_k^2 + Q_k^2)$ ,  $k = 1, \dots, 4$  are the actions of the normal modes. We now write this normal form Hamiltonian in terms of the

slow actions  $J_s$  and  $J_{sp}$ , the two constant actions  $J_c, J_d$  and the slow angles  $\theta_s$  and  $\theta_{sp}$  :

$$\begin{aligned}
H_n = & \epsilon_l + \frac{d}{2}\epsilon_l^2 + \frac{1}{2}d(3 + \alpha)^2 k^2 (3J_s^2 + 3J_{sp}^2 - 4J_s J_{sp} + J_c J_s - 2J_c J_{sp}) \\
& \frac{d1}{8} \sqrt{J_1 J_2 J_3 J_4} \cos(\theta_{sp} + \theta_s) \\
& + \frac{d2}{8} \sqrt{J_1 J_2^2 J_3} \cos(\theta_s) + \frac{d3}{8} \sqrt{J_2 J_3^2 J_4} \cos(\theta_{sp})
\end{aligned} \tag{A10}$$

where the linear energy is

$$\epsilon_l = \Omega_3 J_c + \Omega_4 J_d - \frac{1}{4}(2 + \alpha)k^3 J_s - \frac{1}{4}(3 + \alpha)k^3 J_{sp} \tag{A11}$$

and  $J_1$  through  $J_4$  are functions of  $J_c, J_d, J_s$  and  $J_{sp}$  through (13) and (14). Finally we mention the symmetry that for large  $\alpha$  if we rescale time by the factor  $1/(3 + \alpha)$  and scale all the actions to the constant action  $J_c$  this normal form will depend only on the parameter  $R = 4d(3 + \alpha)J_c/k$ . In other words all the 1234 normal forms with the same  $R$  are equivalent, independent of  $\alpha$ .

Acknowledgement: The authors would like to acknowledge the support of Office of Naval Research Grant N00014-89-J-1097 and National Science Foundation Grant ECS 9217324

## References

- [1] E. Fermi, J. Pasta, and S. Ulam, in: *Collected Papers of E. Fermi*, edited by E. Segre (University of Chicago, Chicago, 1965).
- [2] J. Tuck, M. Menzel, *Adv. Math.* 9, 399 (1972).
- [3] J. Ford, *Journal of Mathematical Physics* 2, 387 (1961).
- [4] E. Atlee Jackson, *Journal of Mathematical Physics* 4, 686 (1963).
- [5] F. M. Izrailev and B. V. Chirikov, *Dokl. akad. Nauk SSSR* 166, 57 (1966)[*Sov. Phys.-Dokl.* 11, 30 (1966)]
- [6] R. Livi, M. Pettini, S. Ruffo, M. Sparpaglione and A. Vulpiani, *Phys. Rev. A* 31, 1039 (1985).
- [7] R. Livi, M. Pettini, Stefano Ruffo, and A. Vulpiani, *Journal of Statistical Physics* 48, 539 (1987).
- [8] Marco Pettini and Marco Landolfi, *Phys. Rev. A* 41, 768 (1990).
- [9] V. I. Arnold, *Mathematical Methods of Classical Mechanics*, appendix 7, Springer-Verlag, N. Y. (1978)
- [10] David S. Sholl, *Analytic Methods for Nonlinear Lattices*, Bachelors Thesis, The Faculties, ANU, March 25, 1991.
- [11] C. G. Goedde, A. J. Lichtenberg, and M. A. Lieberman, *Physica D* 59, 200 (1992).
- [12] Boris V. Chirikov, *A Universal Instability of Many-Dimensional Oscillator Systems*, *Physics Reports* 52, (1979).

## Figure Captions

figure 1 : Domain of slow actions at  $J_d = 0$ .

figure 2 : Surfaces of section of averaged 1234 system with two slow angles for six initial conditions.

figure 3 : Average mode energy after  $t = 12000/\gamma k^2$ ,  $R = 2.9$ .

figure 4 :  $(n_{ef} - 1)/N$  versus  $\gamma k^2 t/3$ , initial condition A and  $N=32$ ,  $\gamma = 3$ ,  $R = 2.9, 5.8$  and  $8.6$  and (solid line)  $\gamma = 6$ ,  $R = 8.6$ .

figure 5 :  $(n_{ef} - 1)/N$  versus  $\gamma k^2 t/3$ , initial condition A,  $\gamma = 3$  and  $R = 5.8, 11.2$  and  $17.2$ .

figure 6 :  $(n_{ef} - 1)/N$  versus  $\gamma k^2 t/3$  for  $R/(N+1) = 0.25$ ,  $N = 16$ (pluses),  $N = 32$ (x),  $N = 64$ (o) and  $N = 128$ (squares).

figure 7 : Effective number of modes versus  $R$  after  $t = 2000(3/\gamma k^2)$ ; pluses  $N = 16$ , crosses  $N = 32$ ; circles,  $N = 64$ .

figure 8 : Logarithm of average energies after  $t = 200(3/\gamma k^2)$  for  $R = 2.9$ ,  $N = 32$ .

figure 9 : Logarithm of average energies after  $t = 200(3/\gamma k^2)$  for  $R = 8.0$ ,  $N = 32$ .

figure 10 : Log of average energies at  $R = 8.0$ ,  $N = 32$  and four consecutive times  $T(3/\gamma k^2)$ ; (a)  $T = 200, n_{ef} = 6.24$ ; (b)  $T = 1000, n_{ef} = 8.67$ , (c)  $T = 4000, n_{ef} = 18.99$ , and (d)  $T = 7800, n_{ef} = 25.48$ .

figure 11 : Average energies after  $t = 6/(\gamma k^2)$  for  $R = 8.0$  and  $N = 64$ . Initial energy in mode 3 ( $\gamma = 3$ ) and initial energy in mode 5 ( $\gamma = 5$ ). The solid line is the geometric progression of (30).

- [13] E. Forest and R. D. Ruth, *Physica D* 43, 105 (1990).
- [14] G. Casati, I. Guarneri, F. M. Izrailev, and R. Scharf, *Phys. Rev. Lett.* 64, 5 (1990).
- [15] F. M. Izraelev, *Phys. Lett. A* 134, 13 (1988) ; *J. Phys. A* 22, 865 (1989).
- [16] R. Livi and S. Ruffo in “Complexity in Physics and Technology” R. V. Mendes, Ed. World Scientific Press (1992).
- [17] G. Benettin, L. Galgani, and A. Giorgilli, *Commun. Math. Phys.* 121, 557 (1989).



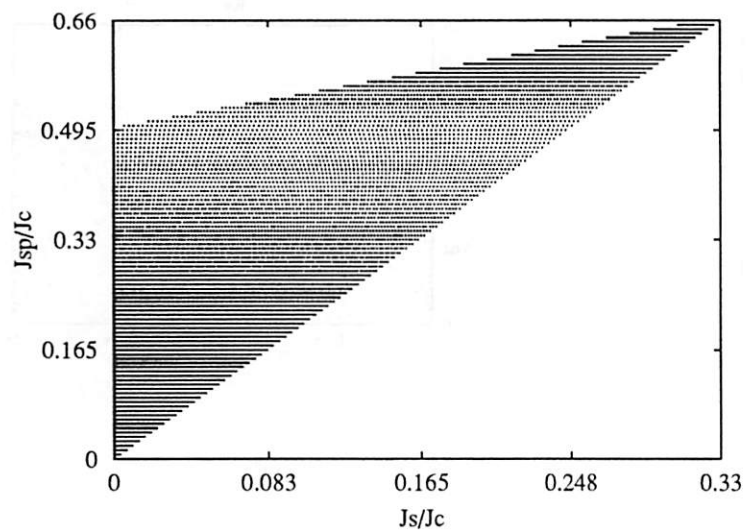


Figure 1: Domain of slow actions at  $J_d = 0$ .

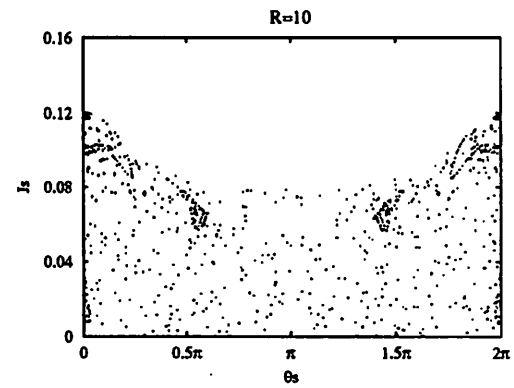
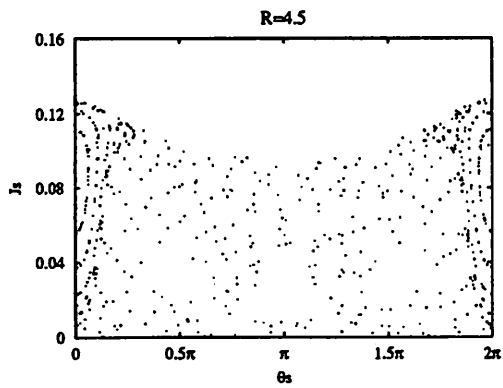
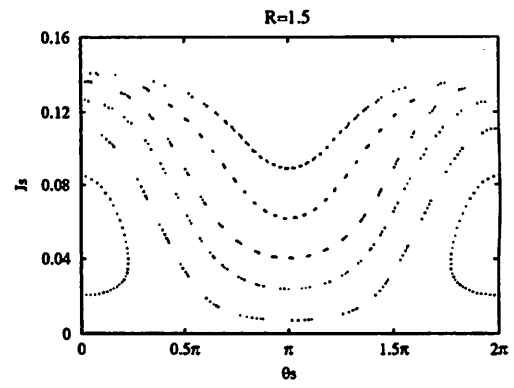
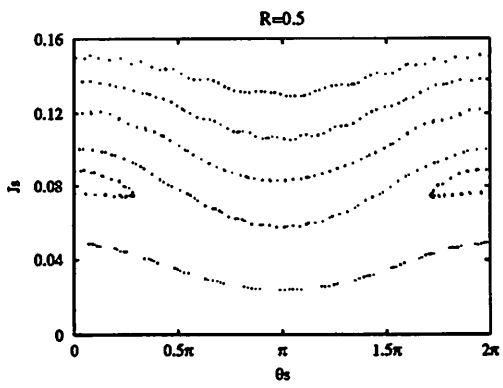


Figure 2: Surfaces of section of averaged 1234 system with two slow angles for six initial conditions.

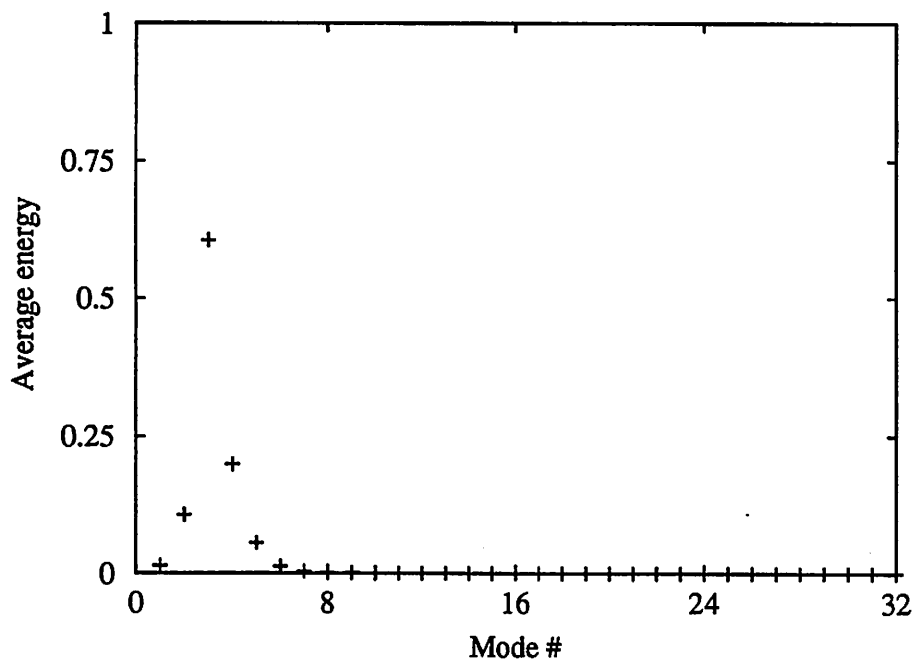


Figure 3: Average mode energy after  $t = 12000/\gamma k^2$ ,  $R = 2.9$ .

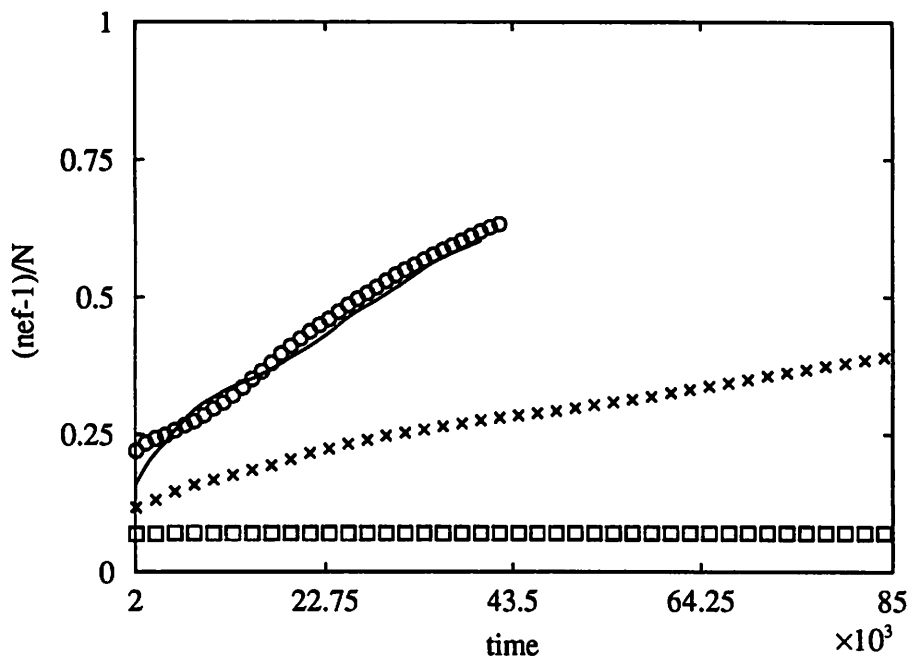


Figure 4:  $(n_{ef} - 1)/N$  versus  $\gamma k^2 t/3$ , initial condition A and  $N=32$ ,  $\gamma = 3$ ,  $R = 2.9, 5.8$  and  $8.6$  and (solid line)  $\gamma = 6$ ,  $R = 8.6$ .

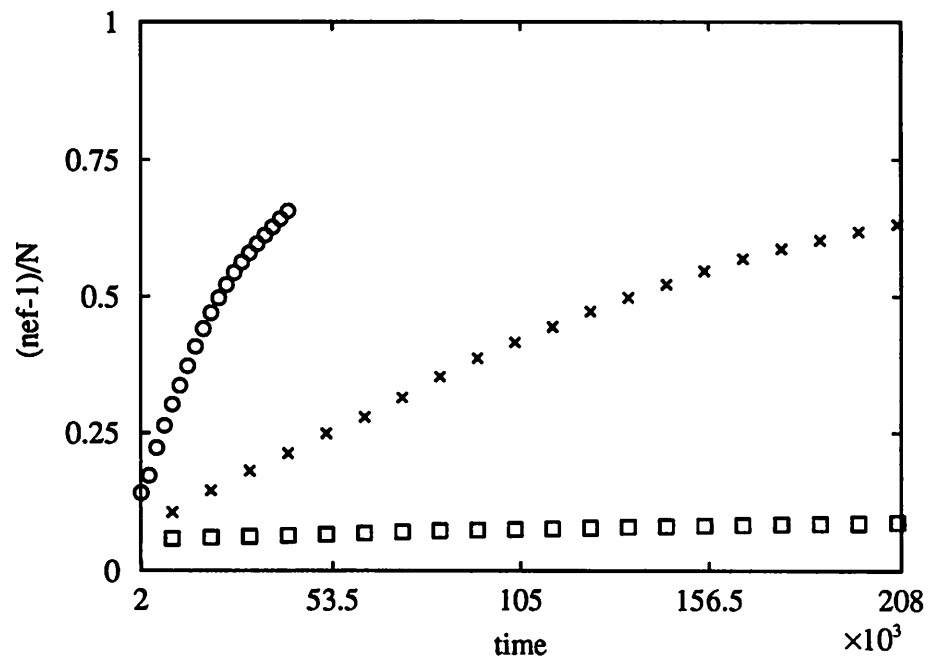


Figure 5:  $(n_{ef} - 1)/N$  versus  $\gamma k^2 t/3$ , initial condition A,  $\gamma = 3$  and  $R = 5.8$ , 11.2 and 17.2

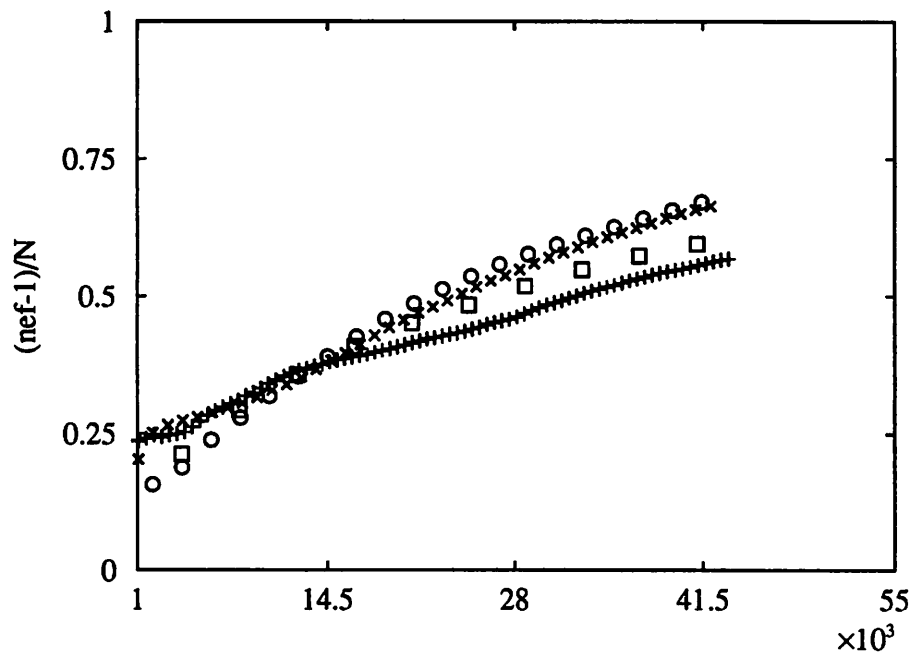


Figure 6:  $(n_{ef} - 1)/N$  versus  $\gamma k^2 t / 3$  for  $R/(N + 1) = 0.25$ ,  $N = 16$ (pluses),  $N = 32$ (x),  $N = 64$ (o) and  $N = 128$ (squares).

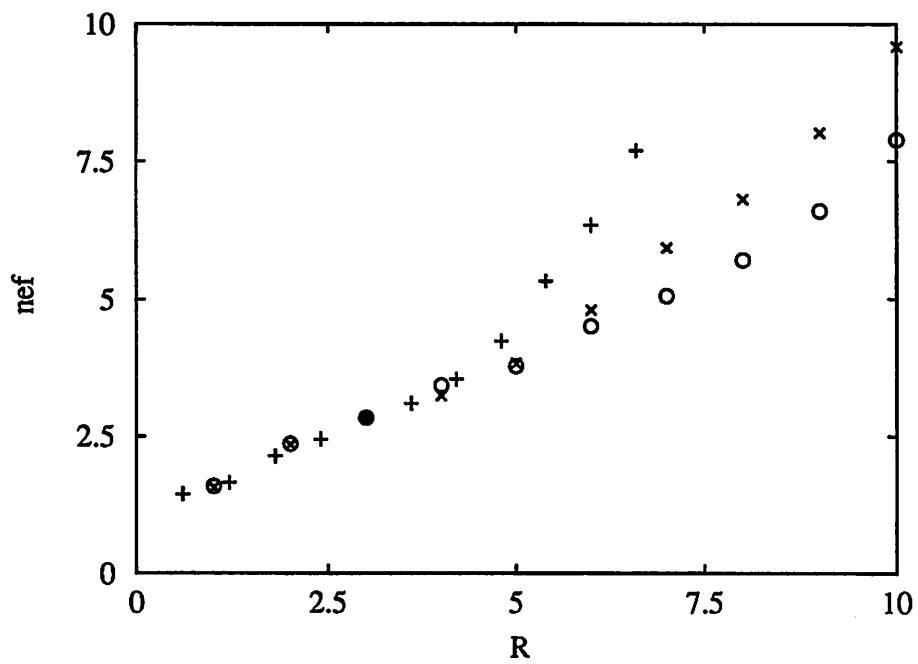


Figure 7: Effective number of modes versus  $R$  after  $t = 2000(3/\gamma k^2)$ ; pluses  $N = 16$  , crosses  $N = 32$  ; circles,  $N = 64$ .

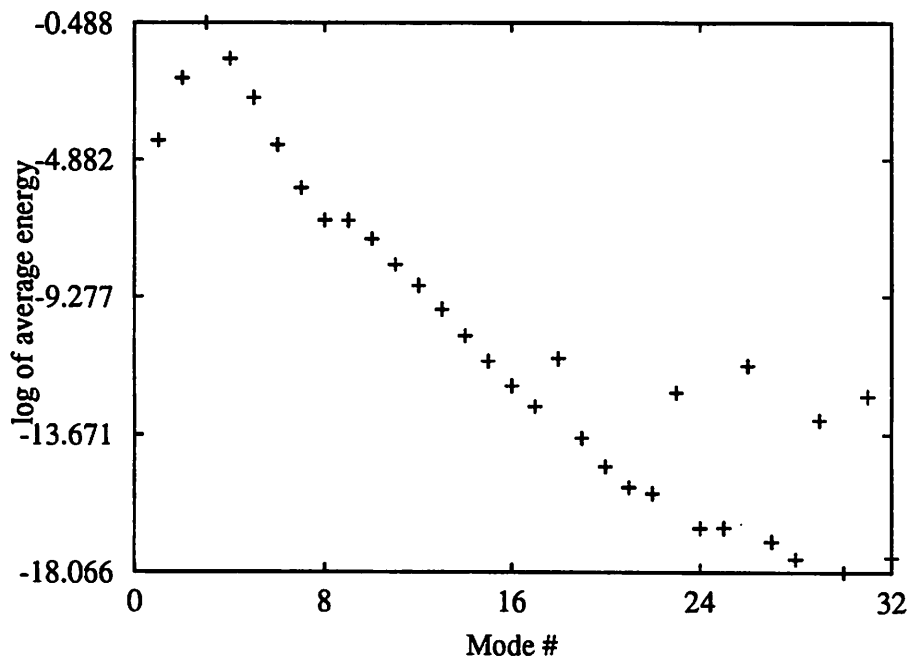


Figure 8: Logarithm of average energies after  $t = 200(3/\gamma k^2)$  for  $R = 2.9$ ,  $N = 32$ .



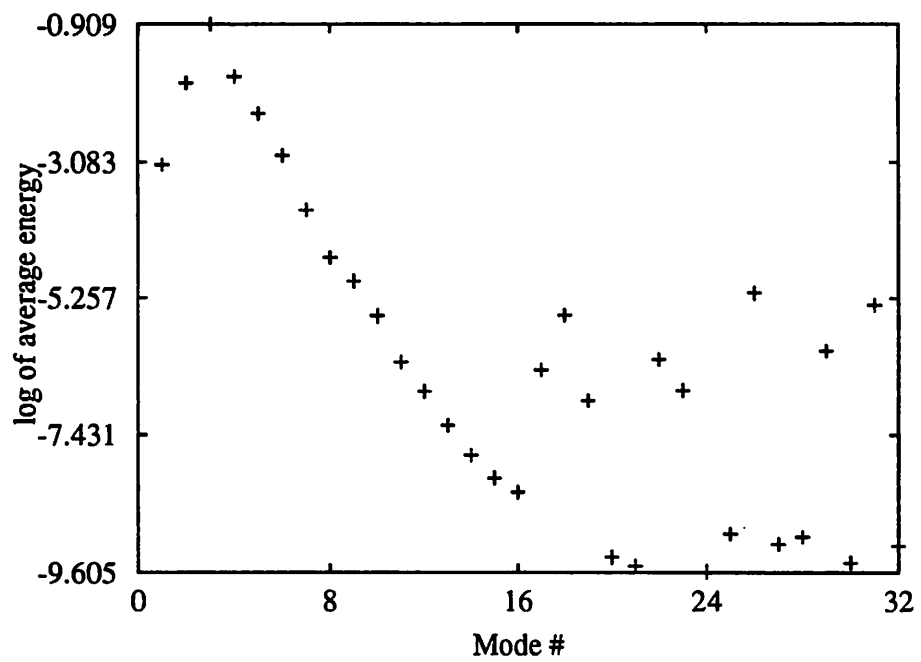


Figure 9: Logarithm of average energies after  $t = 200(3/\gamma k^2)$  for  $R = 8.0$ ,  $N = 32$ .

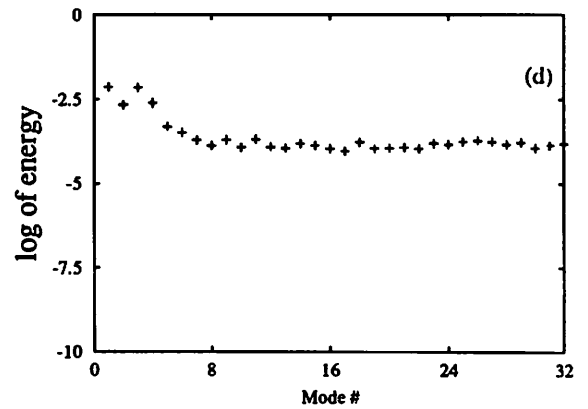
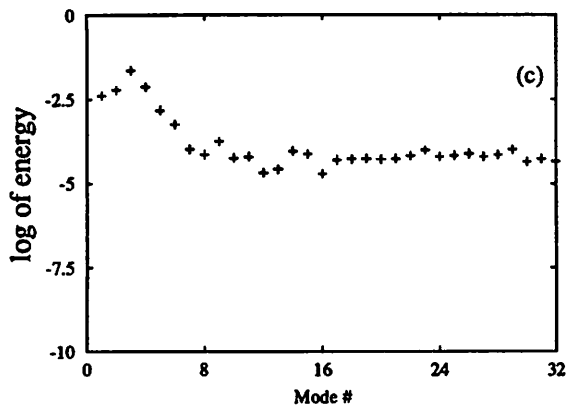
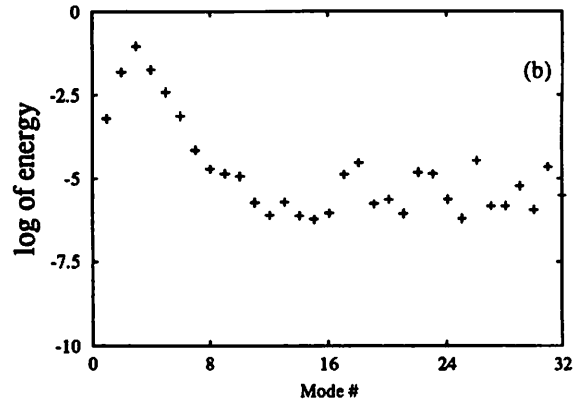
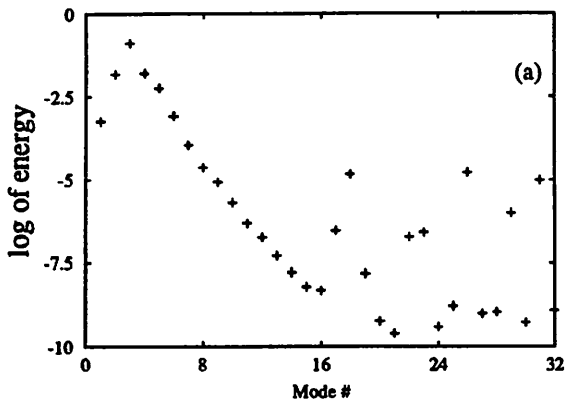


Figure 10: Log of average energies at  $R = 8.0$ ,  $N = 32$  and four consecutive times  $T(3/\gamma k^2)$ ; (a)  $T = 200$ ,  $n_{ef} = 6.24$ ; (b)  $T = 1000$ ,  $n_{ef} = 8.67$ , (c)  $T = 4000$ ,  $n_{ef} = 18.99$ , and (d)  $T = 7800$ ,  $n_{ef} = 25.48$ .

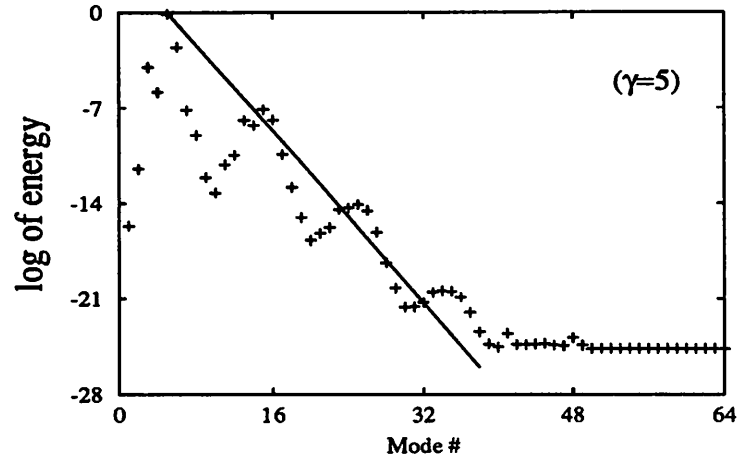
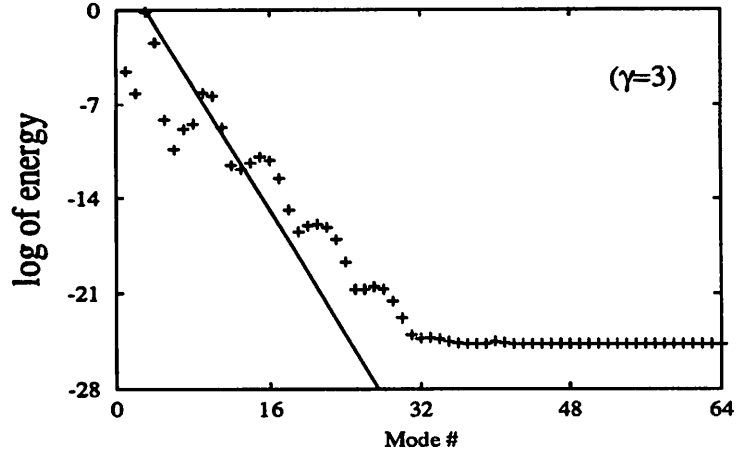


Figure 11: Average energies after  $t = 6/(\gamma k^2)$  for  $R = 8.0$  and  $N = 64$ . Initial energy in mode 3 ( $\gamma = 3$ ) and initial energy in mode 5 ( $\gamma = 5$ ). The solid line is the geometric progression of (30)